THE JOURNAL OF PHYSICAL CHEMISTRY A
A JOURNAL OF THE AMERICAN CHEMICAL SOCIETY

pubs.acs.org/JPCA

Article

Chemistry and Photochemistry of Pyruvic Acid at the Air−Water Interface

Published as part of The Journal of Physical Chemistry virtual special issue "Emily A. Carter Festschrift".

Keaten J. Kappes, Alexandra M. Deal, Malte F. Jespersen, Sandra L. Blair, Jean-Francois Doussin, Mathieu Cazaunau, Edouard Pangui, Brianna N. Hopper, Matthew S. Johnson, and Veronica Vaida*

Cite This: *J. Phys. Chem. A* 2021, 125, 1036−1049

Read Online

ACCESS | Metrics & More | Article Recommendations | Supporting Information

ABSTRACT: Interfacial regions are unique chemical reaction environments that can promote chemistry not found elsewhere. The air−water interface is ubiquitous in the natural environment in the form of ocean surfaces and aqueous atmospheric aerosols. Here we investigate the chemistry and photochemistry of pyruvic acid (PA), a common environmental species, at the air−water interface and compare it to its aqueous bulk chemistry using two different experimental setups: (1) a Langmuir−Blodgett trough, which models natural water surfaces and provides a direct comparison between the two reaction environments, and (2) an atmospheric simulation chamber (CESAM) to monitor the chemical processing of nebulized aqueous PA droplets. The results show that surface chemistry leads to substantial oligomer formation. The sequence begins with the condensation of lactic acid (LA), formed at the surface, with itself and with pyruvic acid, and LA + LA − H_2O and LA + PA − H_2O are prominent among the products in addition to a series of higher-molecular-weight oligomers of mixed units of PA and LA. In addition, we see zymonic acid at the surface. Actinic radiation enhances the production of the oligomers and produces additional surface-active molecules known from the established aqueous photochemical mechanisms. The presence and formation of complex organic molecules at the air−water interface from a simple precursor like PA in the natural environment is relevant to contemporary atmospheric science and is important in the context of prebiotic chemistry, where abiotic production of complex molecules is necessary for abiogenesis.

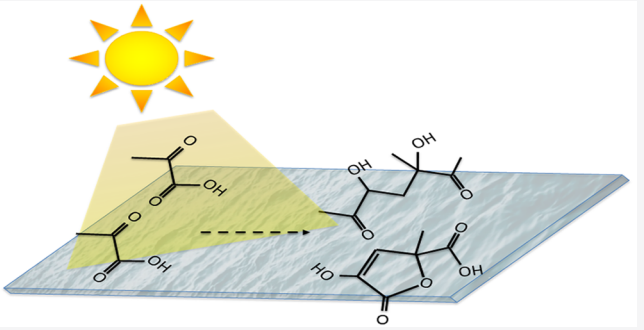

INTRODUCTION

Heterogeneous chemistry occurring in aerosols, clouds, and fogs and at the ocean surface is significant in the natural environment, affecting atmospheric chemistry and climate.[1−9] In the environment, heterogeneous processing occurs at surfaces and interfaces, which provide unique reaction conditions where chemistry proceeds by different mechanisms than in bulk phases.[2,3,5,8−18] These unique reaction conditions could be caused by gradients in concentrations, molecular alignment, water activity, and electric fields at a surface, perturbations to chromophores, or ionization states that differ from those in bulk solution.[8,19−21] Globally distributed aerosols and cloud droplets have an enormous collective surface area.[3,11,22] In fact, the total surface area of aerosols is greater than the combined surface area of all of Earth's bodies of water[23] and provides salient reaction locations in environmental chemistry.[3,8,9,24−26]

Aqueous aerosols have additionally been proposed to be effective prebiotic chemical reactors.[11,13,14,27−31] Formed via wind action at the ocean surface, marine aerosols contain organic material found on the ocean surface.[3,11,27,32] The ocean surface collects and concentrates hydrophobic species from the bulk ocean, the atmosphere, hydrothermal vents, and extraterrestrial infall and then emits these species as sea spray aerosol.[11,27,31] Marine aerosols therefore likely contained the monomeric precursors for complex biomolecules that are thought to have been extant on prebiotic Earth.[27,30] Specifically, the surface of an aerosol provides an environment that is water-restricted and in which organics from the sea-surface microlayer (SML) self-assemble into a monolayer where the molecules are aligned and concentrated.[3,8,11,27,30,33]

The realization that water surfaces can host unique environmental chemistry motivated investigations of organic molecules at the air−water interface.[3,8,24,25,34−42] Surface-specific methods were needed for these studies. For example,

Received: October 7, 2020
Revised: January 9, 2021
Published: January 21, 2021

https://dx.doi.org/10.1021/acs.jpca.0c09096
J. Phys. Chem. A 2021, 125, 1036−1049

nonlinear spectroscopy provided useful information regarding the structure, ion partitioning, and orientation of surfactants at the air−water interface,[43−54] while time-of-flight secondary ion mass spectrometry (ToF-SIMS) offered relatively straightforward molecular identification at the interfacial region.[37,55−59] However, with a few notable exceptions of dark[12,56,60] and photochemical[17,18,37,57,61−66] reactions, relatively little is known about the chemistry and photochemistry of organic species on water and the partitioning of products from the bulk to the surface of water.

In this study, we investigate the chemistry of pyruvic acid (PA) at the surface of water, as it provides an example of a relatively small surfactant molecule with multiple conformers and environment-specific reactivity. PA is naturally found in the gas phase, atmospheric aerosols, polar ice, and precipitation from both direct emission and isoprene oxidation.[67−70] Its multiphase environmental processing is therefore of interest in many facets of atmospheric research, especially as it can alter the chemical and optical properties of atmospheric particles.[3,17,27] The deprotonated form of pyruvic acid, pyruvate, has a long history in biology, including a central role in both aerobic and anaerobic metabolism on modern Earth, where it is oxidized to acetyl CoA or reduced to lactate, respectively. PA may have also contributed to abiogenesis as part of a rudimentary metabolism,[71−76] as it likely would have been available on prebiotic Earth through either abiotic synthesis[71] or delivery by meteorites.[72] Griffith et al.[73] further pointed to the prebiotic relevance of PA by demonstrating its photochemical production of the modern metabolites acetoin and lactic acid as well as molecules larger and more complex than PA.

Previous studies of the gas- and aqueous-phase chemistry of PA are the foundation of this work. The chemistry of PA in the gas phase has been extensively studied.[77−86] Unlike most organics, oxidation of PA by $^{\bullet}OH$ or HO_2 is slow, and therefore, its atmospheric fate is determined by the direct absorption of sunlight by PA and the subsequent photochemical reactions.[81,87] Gas-phase photolysis of PA occurs on the singlet manifold, mainly producing CO_2 and methylhydroxycarbene, which isomerizes to acetaldehyde.[85,86,88,89] This process occurs with a quantum yield of 1 at low buffer gas pressures.[77,82,85,86]

The mechanisms of aqueous photochemistry of PA proceed through a different pathway than the gas-phase photolysis.[89−99] Briefly, diffuse UV radiation can excite a PA molecule to its S_1 state, which then undergoes intersystem crossing to the T_1 state and generates organic radicals, finally resulting in several complex oligomers depending on the specific reaction conditions. The effects of concentration, pH, and O_2 on the reaction mechanism, product yields, and array of products in aqueous phase have all been described.[37,57,63,73,90−93,96−103] Interpreted using the gas- and aqueous-phase photochemistry of pyruvic acid, the multiphase chemistry of PA has been studied, highlighting the formation of oligomers and consequently the construction of chemical complexity with sunlight.[17] Results from a study of the multiphase chemistry of pyruvic acid indicated that the air−water interface plays a significant role in promoting chemistry not possible in either the gas or bulk aqueous phase.[17] Another investigation reached a similar conclusion by modifying their sample preparation methods to simulate the difference between bulk and interfacial photochemistry and observed higher-molecular-weight compounds to be enhanced at the surface relative to the bulk.[37]

In this study, we examine the chemistry and photochemistry of pyruvic acid at the air−water interface. We use a combination of Langmuir−Blodgett troughs and simulation chamber studies to model environmental air−water interfaces, including the surface of nebulized microdroplets. These studies aim to elucidate the role that the water surface plays in the multiphase chemistry of pyruvic acid. Chemical and photochemical experiments provide key distinctions between reactions at the air−water interface and the bulk aqueous solutions. Comparison of the results from chemistry conducted on a flat air−water interface (Langmuir−Blodgett trough) with the results from nebulized droplets in an environmental simulation chamber (CESAM)[17,79,104] highlight the chemistry specific to the air−water interface. Finally, we comment on the importance of pyruvic acid's unique chemistry at the air−water interface to modern and prebiotic environmental chemistry.

METHODS

Sample Preparation. Pyruvic acid (Sigma-Aldrich, 98%) was vacuum-distilled ($P < 1$ mbar) with stirring and heating ($T < 70$ °C) to remove impurities. Nuclear magnetic resonance spectroscopy (NMR) was used to demonstrate the purity of pyruvic acid (see the Supporting Information for details and Figure S1). The purified pyruvic acid was stored at 2 °C in the dark and used within 1 month of distillation to minimize dark aging processes that could generate oligomeric species.[17,92,99,105] Aqueous solutions of pyruvic acid were prepared in 18.2 MΩ (3 ppb total organic carbon) water, followed by sonication until the PA was fully dissolved. The pH values of aqueous solutions were left unadjusted and were determined using a Corning 320 pH meter. All glassware was cleaned in a KOH/EtOH base bath and rinsed with water and methanol (Fisher Chemical, 99.8%) prior to use.

Langmuir−Blodgett Trough. A custom-built Langmuir trough (52 cm × 7 cm × 0.5 cm) used previously in our group[12,19,106−111] is briefly summarized here. It is made of polytetrafluoroethylene (PTFE) and equipped with two computer-controlled NIMA (KSV-NIMA, Finland) PTFE barriers to restrict the available surface area. A Wilhelmy balance was used to monitor the surface pressure of the aqueous solution in the trough as the barriers compress molecules at the air−water interface, providing surface pressure−area isotherms and therefore insight into the surface activity of the molecules in solution. For example, isotherms of an aqueous PA solution before and after exposure to UV radiation are provided in Figure S2.

A Kibron LayerX (134) dip coater attached to the custom-built Langmuir trough was used to transfer molecules residing at the surface of the aqueous subphase to a solid substrate (glass slide) for surface-specific species collection. The dip coater moved a clean glass slide into the aqueous subphase and withdrew to its original starting position. This process was repeated for a total of 10 cycles, while the trough barriers compressed the surface area such that the surface pressure was held roughly constant. Methanol (1 mL) was used to extract the organic film collected on the glass slide. Special care was taken to prevent solvent evaporation in order to avoid drying-induced chemistry. The resulting methanol solution was analyzed with negative-mode electrospray ionization mass spectrometry (ESI-MS). Peak assignments were made by comparing theoretical mass-to-charge ratios for known or

https://dx.doi.org/10.1021/acs.jpca.0c09096
J. Phys. Chem. A 2021, 125, 1036−1049

expected products to experimental mass-to-charge ratios. The mass accuracy for most assignments was within ∼10 ppm. Additional ESI-MS details are included in the Supporting Information.

The aqueous subphase in Langmuir−Blodgett trough experiments consisted of 100 mM pyruvic acid (pH ∼1.8), which reflects environmental conditions and previous work.[63,67] Samples were collected simultaneously from the surface via the dip coater and from the bulk by syringe.

Photochemical Studies. Photochemical experiments were performed by irradiating the entire aqueous sample in the Langmuir trough with UV light. The light source consisted of Waveform Lighting light-emitting diode strips (realUV LED Strip Lights; 365 nm) adhered to the trough cover, ensuring irradiation of the entire trough surface and subphase. The spectral output of the LEDs is shown in Figure 1, overlaid upon the absorbance spectrum of 100 mM aqueous pyruvic acid (pH ∼1.8). The LEDs emitted radiation between 355 and 395 nm with a λ_{max} of ∼370 nm, which overlapped with the tail end of the photochemically relevant (n−π^*) transition of pyruvic acid, as shown in Figure 1. Solar simulators commonly used in other photochemical experiments, including aqueous solution studies in this group,[73,92,94,99,102,112,113] provide radiation across a larger portion of the S_1 PA absorption, as shown in Figure 1. Therefore, a comparison between the bulk photochemistry of PA irradiated with the LEDs and with the Xe arc lamp is worthwhile.

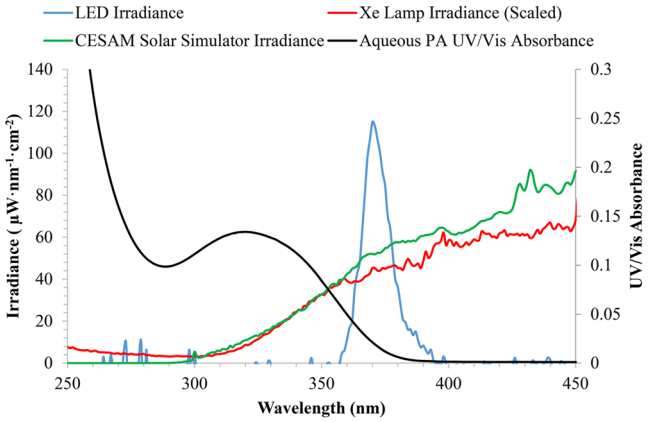

Figure 1. Comparison between the spectral outputs of the photochemical sources used in these experiments: LEDs (blue), a Pyrex-filtered 450 W Xe arc lamp (scaled; red), and the CESAM Pyrex-filtered solar simulator (green). These are overlaid on the absorbance spectrum of aqueous pyruvic acid (100 mM, pH ∼1.8) (black). The Xe arc lamp output was scaled down by a factor of 11.

Light Source Comparison. Bulk aqueous photolyses of 100 mM PA were performed with LEDs on the Langmuir trough and with a 450 W Xe arc lamp (the spectral output is shown in Figure 1) to compare the photoproducts obtained with the two light sources. The experimental method utilizing the 450 W Xe arc lamp is described in Photochemical Reaction Cell. Each light source produced the expected major products, 2,4-dihydroxy-2-methyl-5-oxohexanoic acid (DMOHA) (m/z = 175) and dimethyltartaric acid (DMTA) (m/z = 177) (see Table 1). Additional photolysis products included acetoin (m/z = 87), acetolactic acid (AcLA) (m/z = 131), and 4-carboxy-2,4-dihydroxy-2-methyl-5-oxohexanoic acid (CDMOHA) (m/z = 219). For both sources, these results were consistent with previous studies, which have described the mechanisms of bulk aqueous PA in detail.[83−85,93,10492,94,99,102,113] While the observed products are the same for both light sources, the normalized ion intensities of the photoproducts are generally smaller in the LED photolysis than in the Xe lamp photolysis. The lower intensity of the photolysis source and the limited overlap between the LED output and PA absorbance spectrum results in a lower photolysis rate, but these factors do not seem to significantly alter the photoproducts observed and therefore the photochemical pathways of PA.

Photochemical Reaction Cell. Photolysis using the solar simulator, for comparison with the LED light source, was performed in a photochemical reaction cell. An aqueous solution of pyruvic acid (100 mM; unadjusted pH ∼1.8) was placed in a glass photochemical reaction cell surrounded by a temperature-controlled water bath at 20 °C. The sample was photolyzed using an unfiltered 450 W Xe arc lamp (Newport) for 2 h with constant nitrogen sparging. Aqueous pyruvic acid samples before and after photolysis for 2 h were analyzed with negative-mode ESI-MS after 1:1 dilution in methanol.

Atmospheric Simulation Chamber (CESAM). A 4.2 m^3 stainless steel atmospheric simulation chamber, CESAM (French acronym for Experimental Multiphasic Atmospheric Simulation Chamber), was used here and in previous studies of gas-phase and multiphase photochemistry of PA to probe the dark chemistry and photochemistry of aqueous pyruvic acid.[17,79,82,104] We discuss the relevant experimental parameters here; a full description of the CESAM facility and analysis

Table 1. Negative-Mode ESI-MS Ion Peaks of Bulk Aqueous 100 mM Pyruvic Acid after 2 h of Photolysis with Two Different Light Sources: A Xe Arc Lamp and LEDs

		m/z			normalized ion intensity[a]	
ion formula, $[M - H]^-$	assigned structure	theor	exptl	mass diff. (ppm)	Xe lamp	LEDs
$C_3H_3O_3^-$	pyruvic acid (PA)	87.0088	87.0077	12.64	100	100
$C_4H_7O_2^-$	acetoin	87.0452	87.0442	11.49	8.6	4.65
$C_5H_7O_3^-$	unassigned	115.0401	115.039	9.56	32.7	18.4
$C_5H_7O_4^-$	acetolactic acid (AcLA)	131.035	131.0342	6.11	36.5	9.47
$C_6H_7O_5^-$	PA + LA − H_2O	159.0299	159.0283	10.06	5.06	3.12
$C_6H_7O_6^-$	parapyruvic acid (PPA)	175.0248	175.0231	9.71	2.14	4.83
$C_7H_{11}O_5^-$	2,4-dihydroxy-2-methyl-5-oxohexanoic acid (DMOHA)	175.0612	175.0605	4.00	228	231
$C_6H_9O_6^-$	dimethyltartaric acid (DMTA)	177.0405	177.0396	5.08	872	596
$C_8H_{11}O_7^-$	4-carboxy-2,4-dihydroxy 2-methyl-5-oxohexanoic acid (CDMOHA)	219.051	219.0501	4.11	6.15	6.82

[a]Intensities are normalized such that the intensity of PA at m/z = 87 is set to 100.

https://dx.doi.org/10.1021/acs.jpca.0c09096
J. Phys. Chem. A 2021, 125, 1036−1049

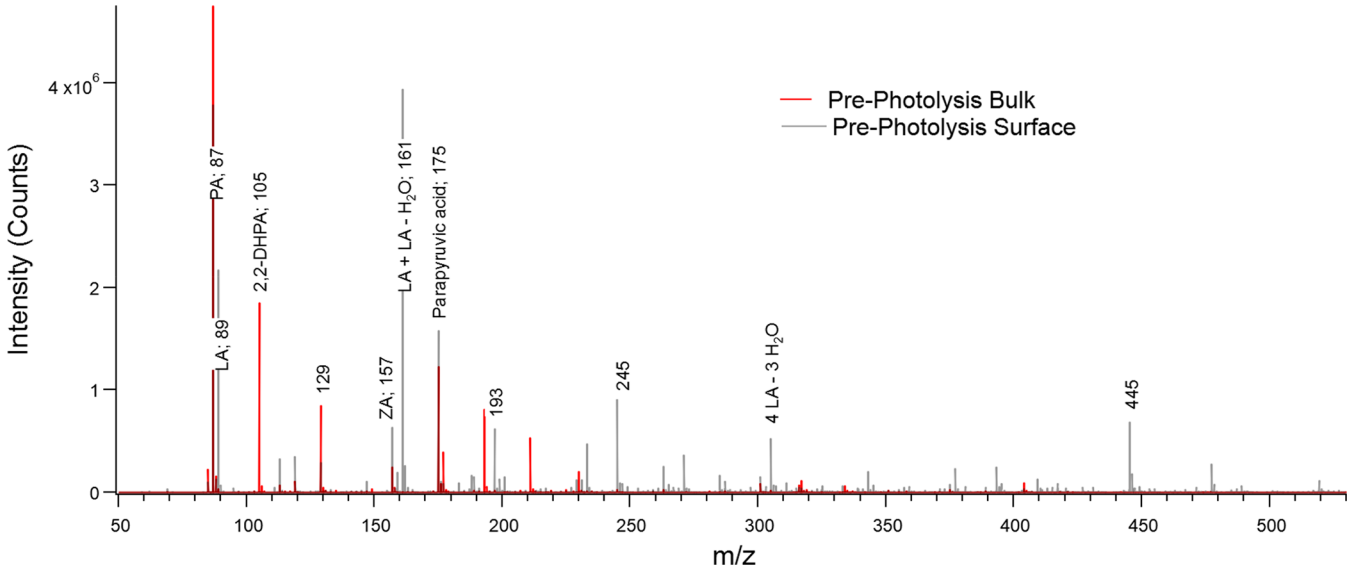

Figure 2. Negative-mode ESI-MS of a 100 mM PA aqueous solution sampled from the bulk (red) and the surface (transparent gray) of a Langmuir−Blodgett trough. Dark-red traces result from overlap between the two defined spectra. Samples were taken immediately after the solution was deposited in the trough. The full ESI-MS ion scan range is shown to demonstrate the increased prevalence of high-molecular-weight species at the surface compared with the bulk.

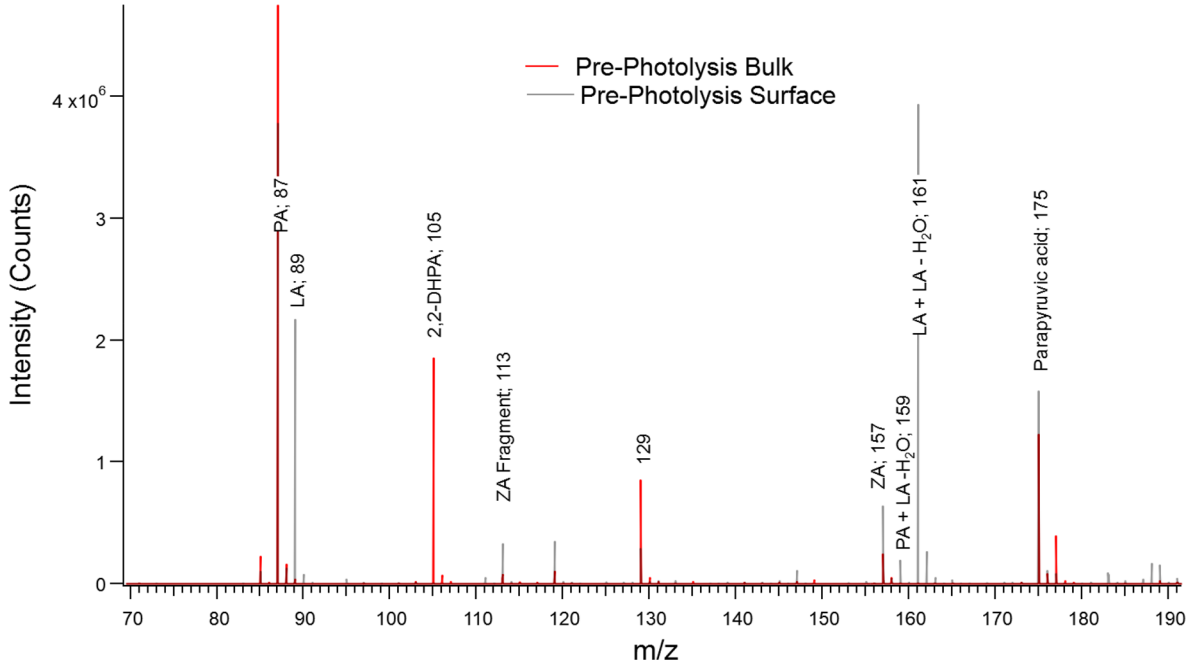

Figure 3. Negative-mode ESI-MS of a 100 mM PA solution sampled from the surface (transparent gray) and the bulk (red) of a Langmuir−Blodgett trough, focusing on the region of lower molecular weight. Dark-red traces result from overlap between the two defined spectra. Samples were taken immediately after the aqueous solution was deposited in the trough. Pyruvic acid (PA) and/or pyruvate are the dominant species in both the surface and the bulk. Lactic acid (LA) or lactate, zymonic acid (ZA), and oligomers of PA and LA are predominantly found at the surface, while the geminal diol of PA, 2,2-dihydroxypropanoic acid (2,2-DHPA) is predominantly found in the bulk. The PA dimer parapyruvic acid (PPA) appears in both the surface and the bulk.

techniques can be found in the papers by Wang et al.[104] and Bregonzio-Rozier et al.[114] In this study, an atomizer (TSI, model 3075) through a diffusion dryer (TSI, model 3062) employed N_2 to aerosolize aqueous droplets of pyruvic acid from an aqueous solution of pyruvic acid into CESAM, conditioned to ∼90% relative humidity (RH) and a temperature of 25 °C and filled to ambient pressure (∼1015 mbar). The nebulization process was continued until the particle mass and number concentrations (measured by a scanning mobility particle sizer) in CESAM were 20 $\mu g/m^3$ and 1×10^5 cm^{-3}, respectively. The geometric mean diameter of aqueous pyruvic acid droplets was 60 nm. Pyruvic acid droplets were photolyzed by irradiation from a solar simulator consisting of three 4 kW high-pressure Xe arc lamps (MH-Diffusion, MacBeam 4000) filtered by 6.5 mm thick Pyrex windows (see Figure 1 for the CESAM solar simulator spectral output).

https://dx.doi.org/10.1021/acs.jpca.0c09096
J. Phys. Chem. A 2021, 125, 1036−1049

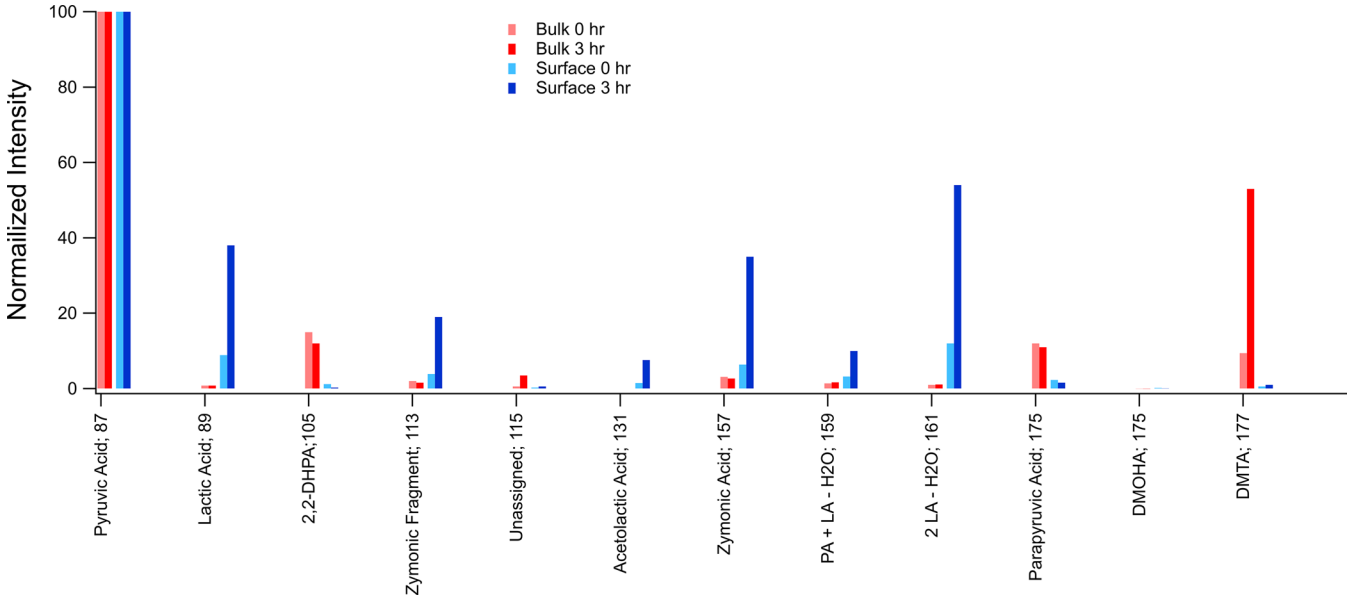

Figure 4. Behavior of selected ESI-MS ion peaks over time for Langmuir−Blodgett trough control experiments. Intensities were normalized such that the intensity of PA at m/z = 87 was set to 100.

The gas-phase species in CESAM were tracked in situ with a proton transfer reaction time-of-flight mass spectrometer (PTR-ToF-MS Series II, Kore Technology) that sampled the air in counterflow, preventing aerosol and droplet sampling. Aqueous pyruvic acid droplets were collected on filters and analyzed postcollection with negative-mode ESI-MS after extraction in methanol. The data presented here are from two different CESAM experiments. We show (1) the PTR-ToF-MS data (Figure 8) from an experiment that took place on 10/17/2018 in which droplets were nebulized from a 300 mM PA solution into CESAM filled with synthetic air and (2) ESI-MS data (Table S3) of a filter-collected sample from a 6/11/2015 experiment in which droplets were nebulized from a 100 mM PA solution into CESAM filled with N_2.

RESULTS

The results of two sets of distinct experiments are presented below. First, we report on the chemistry and photochemistry of PA taking place at the air−water interface obtained using a Langmuir−Blodgett trough and compare it to that which occurs in the bulk. Then we compare and contrast the chemistry of PA in the Langmuir trough to its chemistry in nebulized droplets using an atmospheric simulation chamber, CESAM.

Langmuir−Blodgett Studies. *Mass Spectrometry Analysis of Interfacial Pyruvic Acid.* Prior to irradiation of a 100 mM PA aqueous solution, an aliquot of the bulk solution was collected, and separately, a Langmuir−Blodgett dipper followed by a methanol wash was used to collect molecules residing at the surface of the solution. Both samples were analyzed after collection via negative-mode ESI-MS. The resulting spectra are shown in Figure 2 and summarized in Table S2. It is immediately apparent that the sample taken from the surface contains significantly more species of relatively high molecular weight. Because the NMR results on the pyruvic acid precursor demonstrate a high degree of purity (see Figure S1) and the high-molecular-weight species are not seen in the bulk, these compounds are oligomers that spontaneously form at the air−water interface and/or are formed in the bulk and then partition to the water surface where we observe them. In fact, the ability of pyruvic acid to form oligomers, such as zymonic acid (ZA), is well-documented.[37,105]

Indeed, ZA was observed at the surface and in the bulk at m/z = 157. Figure 3 focuses on the lower-molecular-weight region of Figure 2 to illustrate additional differences between the surface and bulk of the PA aqueous solution. Here we see a strong peak at m/z = 89, corresponding to lactic acid (LA) or lactate, at the surface but not in the bulk. We considered the possibility that lactic acid is merely a contamination; however, NMR of our purified PA was not able to identify any LA contamination. Additionally, in an aging experiment where 100 mM aqueous PA was allowed to sit on the trough for 3 h (see Figure 4 and Table S1) there was LA on the surface of the solution but not in the bulk at time = 0 h. After 3 h of sitting on the trough, there was a significant increase in LA at the surface but no such increase in the bulk. If LA were only a product of our collection or analysis method, the LA signal should not increase with time. Furthermore, LA is a water-soluble molecule, so we would expect any LA contaminant also to be observed in the bulk, yet it was detected only at the interface.

The most prominent peak observed at the surface, though not in the bulk, is at m/z = 161, which may correspond to the condensation product of two lactic acid monomers. At m/z = 159 we also observe the presence of what may be PA + LA − H_2O. In fact, as listed in Table S2, many of the higher-molecular-weight species shown in Figure 2 correspond to the myriad possible oligomers potentially formed from combinations of LA and PA molecules and the requisite loss of water molecules.

Another interesting difference between the aqueous PA surface and bulk reaction environments is revealed by the peak found only in the bulk at m/z = 105: the diol form of PA. As the diol is likely more soluble than the keto form because of its additional −OH groups and probably less likely to form at or partition to the surface given the water-restricted nature of the interface, it seems reasonable the diol is not observed at the

https://dx.doi.org/10.1021/acs.jpca.0c09096
J. Phys. Chem. A 2021, 125, 1036−1049

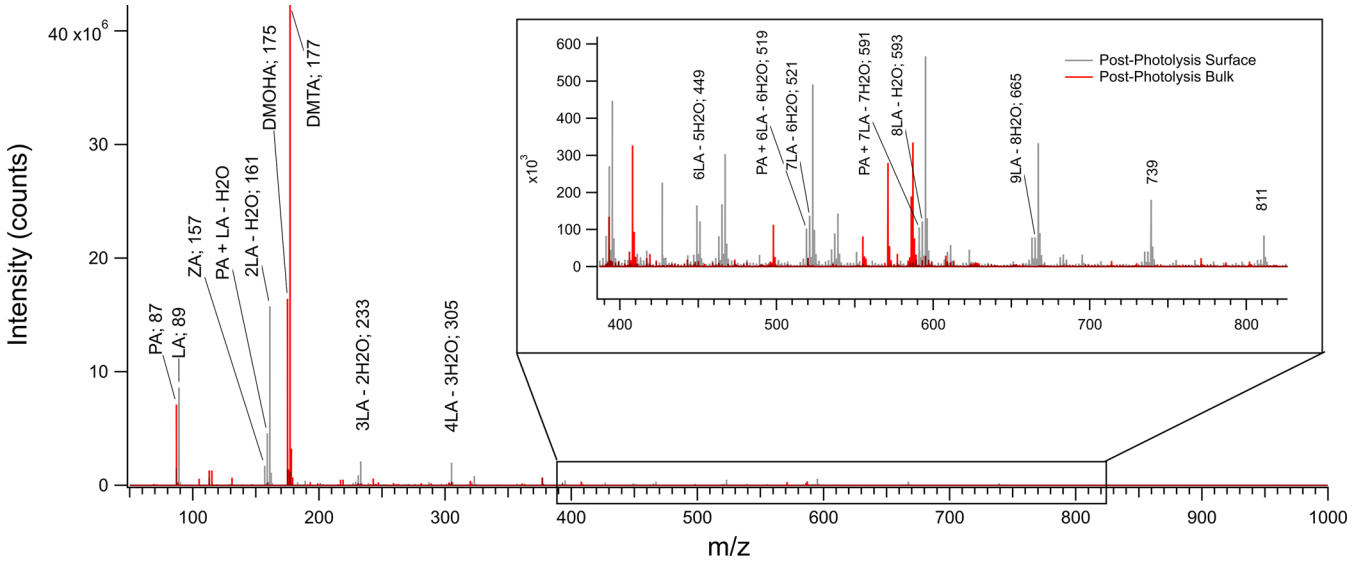

Figure 5. Negative-mode ESI-MS of 100 mM aqueous PA sampled from the Langmuir−Blodgett trough surface (transparent gray) and bulk (red) after 3 h of irradiation. Dark-red traces result from overlap between the two defined spectra.

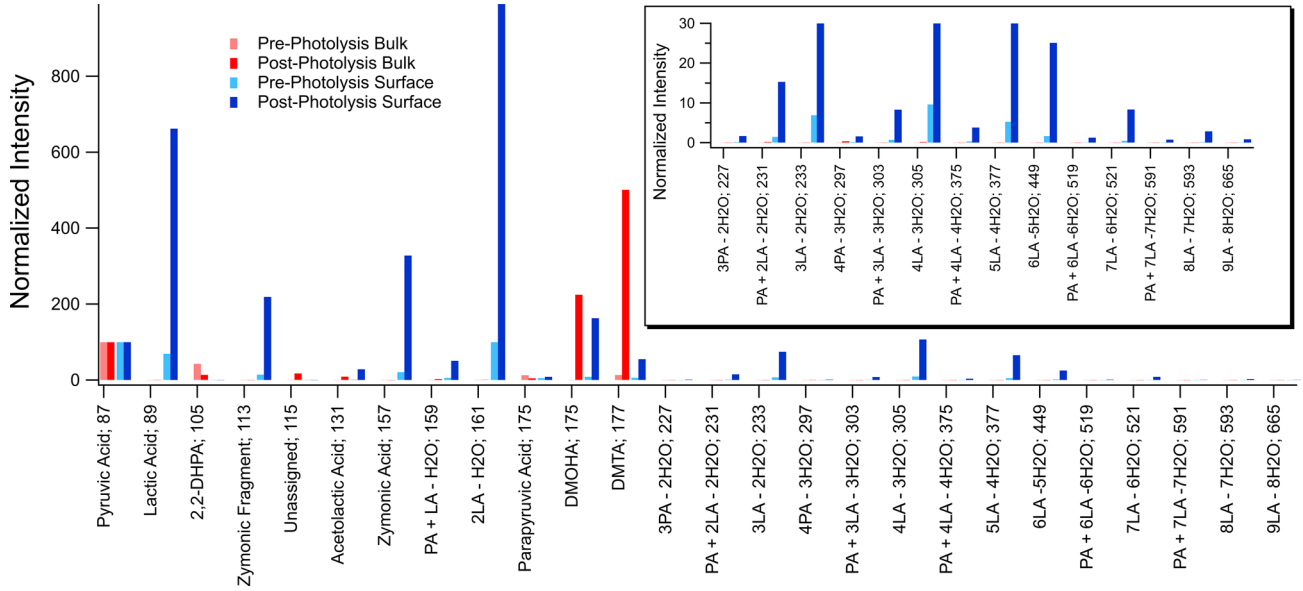

Figure 6. Behavior of selected ESI-MS ion peaks for 100 mM PA before and after photolysis sampled in the bulk and on the solution surface. Intensities were normalized such that the intensity of PA at m/z = 87 was set to 100.

surface. Furthermore, we do not expect that washing the diol in methanol, as performed on all of the samples collected from the water surface, would force the diol back into the keto form of PA.[115,116]

Photochemistry of Pyruvic Acid at the Surface of Water. A Langmuir−Blodgett trough was coupled to photochemistry-inducing LEDs and used to photolyze aqueous PA solutions. After irradiation of a 100 mM solution of aqueous PA in the trough for 3 h, an aliquot of the bulk solution was collected from the trough, and a Langmuir−Blodgett dipper was used to collect molecules residing at the surface of the solution. Negative-mode ESI-MS was used to analyze both samples, and the results are shown in Figure 5 and summarized in Table S2 and Figure 6.

At the surface pre- and postphotolysis, the most prominent signals arise from PA (m/z = 87), LA (m/z = 89), and the host of PA, LA, and PA/LA oligomers at m/z = 157 (ZA), 159, 161, 231, 303, etc. These oligomeric species are more prevalent after irradiation. Zymonic acid is well-known to form in the dark,[105] but these experiments also show dark production of LA and other oligomers. Additionally, formation of the well-documented aqueous PA photoproducts[37,63,80,90,92,97,99,101,102,113] is observed on the surface postirradiation, the most prominent of which include acetolactic acid (m/z = 131), DMOHA (m/z = 175), and DMTA (m/z = 177). The mechanism for the formation of these species in the bulk aqueous phase has been previously reported.[17,63,73,92,99]

Figure 7 compares the postphotolysis mass spectrum taken from the bulk to that taken from the surface of a Langmuir−Blodgett trough. Though LA is a well-known photolysis product of PA in aqueous solution, the most striking differences in the postphotolysis mass spectra are the observation of LA and PA/LA oligomers at the surface but

https://dx.doi.org/10.1021/acs.jpca.0c09096
J. Phys. Chem. A 2021, 125, 1036−1049

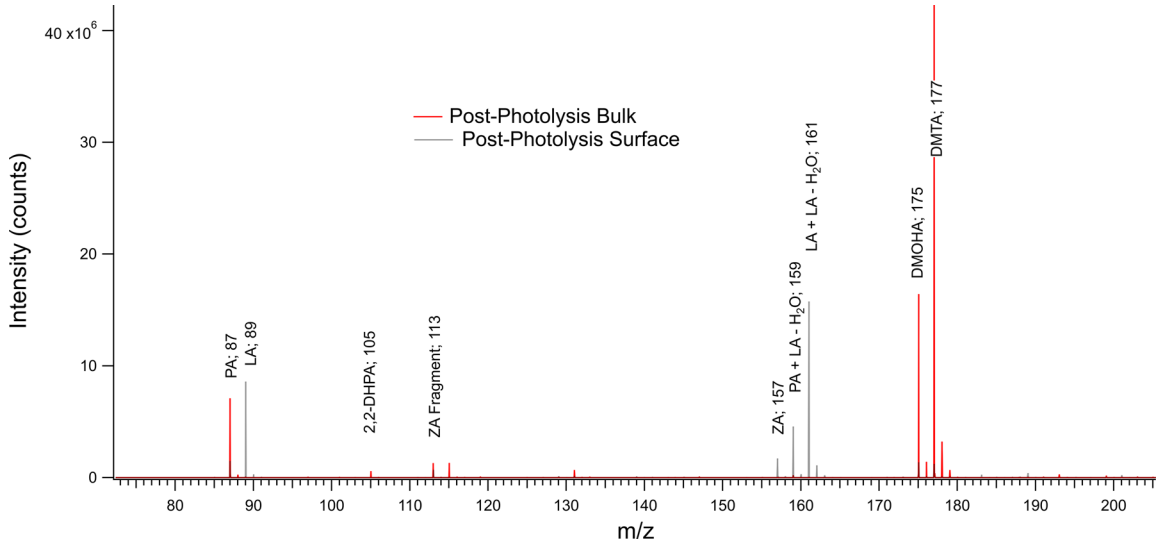

Figure 7. Negative-mode ESI-MS of a 100 mM PA aqueous solution after 3 h of irradiation with samples taken from the surface (transparent gray) and bulk (red) of a Langmuir−Blodgett trough. Dark-red traces result from overlap between the two defined spectra. The expected photolysis products 2,4-dihydroxy-2-methyl-5-oxohexanoic acid (DMOHA) and dimethyltartaric acid (DMTA) are found primarily in the bulk. Zymonic acid (ZA), lactic acid (LA), and oligomers of PA and LA are found primarily at the surface.

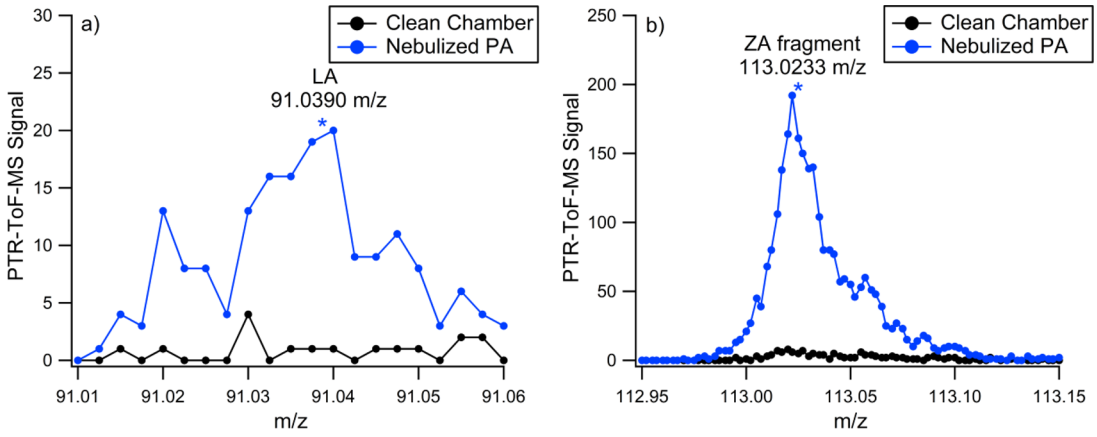

Figure 8. PTR-ToF-MS ion peaks for (a) lactic acid (LA) (m/z = 91.0390) and (b) zymonic acid (ZA) ($[M + H - H_2O - CO]^+$ m/z = 113.0233) fragments in the nebulized pyruvic acid CESAM experiment. The mass spectra are shown as lines with solid circle markers and are colored black for the clean chamber and blue for nebulized pyruvic acid in the chamber.

not in the bulk solution. In the bulk, the major species are the photoproducts DMOHA and DMTA. While they are also observed at the interface, the relative concentrations are much greater in the bulk than at the surface.

Overall, the chemistry and photochemistry of PA at the air−water interface is defined by the formation of lactic acid and/or lactate and several oligomers comprising various ratios of PA to LA monomers. The production of expected PA photoproducts such as DMOHA and DMTA may be limited at the surface compared with the bulk.

Simulation Chamber (CESAM) Studies of Nebulized Aqueous PA Microdroplets. Aqueous PA droplets in CESAM, formed via nebulization of 100 mM aqueous PA, were filter-collected before photolysis and analyzed with ESI-MS. The results were compared with ESI-MS measurements of the bulk sample prepared in the photochemical reaction cell experiment before photolysis and can be seen in Table S3. The relative amounts of some species were much larger in the PA droplets than observed in the bulk, including acetoin (m/z = 87), LA (m/z = 89), ZA (m/z = 157), PA + LA − H_2O (m/z = 159), and parapyruvic acid (PPA) (m/z = 175). These results suggest that dark chemistry not seen in bulk aqueous solutions can occur in PA droplets, which collectively have a large surface area to volume ratio.

Support for the formation of lactic and zymonic acids at the droplet surface can be seen in Figure 8, where PTR-ToF-MS signals of their ions are shown as PA is nebulized into CESAM. The ZA fragment signal ($[M + H - H_2O - CO]^+$ at m/z = 113)[17] greatly increased as PA was nebulized into the chamber. The fragment signal at m/z = 113 is used as a marker for zymonic acid instead of its parent peak at m/z = 159, as the former is seen with higher intensity. However, the two PTR-ToF-MS ion signals representative of the acid follow the same time trend. Lactic acid (m/z = 91) also increased during PA nebulization, though not as significantly. Neither of these PTR-ToF-MS signals were observed in the gas-phase dark aging experiments of PA,[79] indicating that the droplets, and more specifically their surface,[14,45] are necessary for this dark production. The particle number and mass concentrations of PA in the multiphase nebulized experiment were 10^5 cm^{-3} and

https://dx.doi.org/10.1021/acs.jpca.0c09096
J. Phys. Chem. A 2021, 125, 1036−1049

Scheme 1. Proposed Mechanism for PA + LA − H_2O Dimer Formation (Pathway B) Compared to the Proposed Mechanism for Zymonic Acid[a] (i.e., PA + PA − H_2O Dimer) Formation[99,102] (Pathway A)

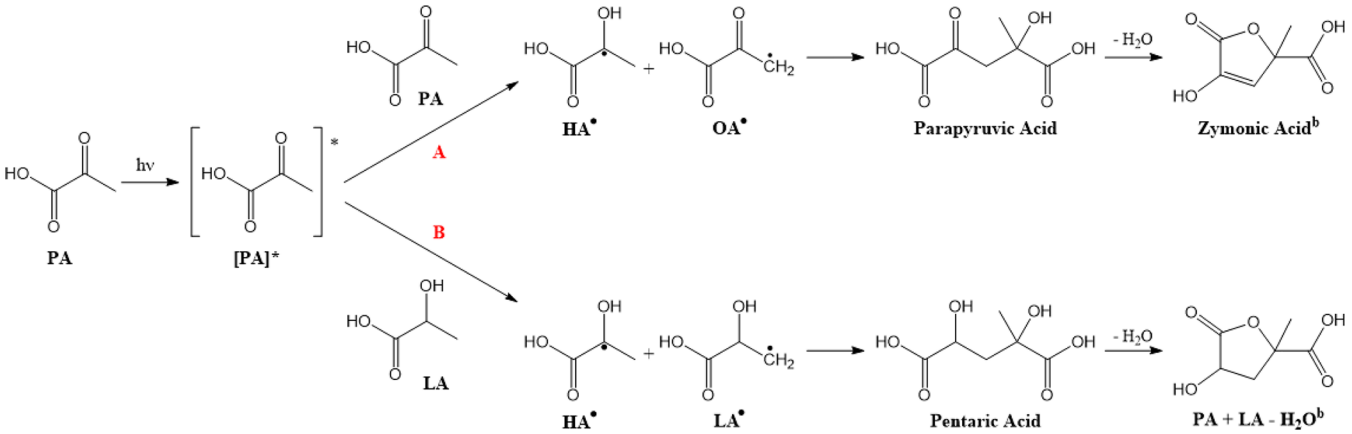

[a]ZA is a known product of both dark and photochemical reactions of PA.[17,105] [b]The final product structures shown here are one of multiple possible stereoisomers for the PA + PA − H_2O and PA + LA − H_2O dimers. See Figure S4 for other potential product structures.

20 μg m^{-3}, respectively, with a number-weighted mean geometric diameter of 60 nm. The average surface area and surface to volume ratio of a PA particle in the experiment were 0.011 μm^2 and 0.1 nm^{-1}, respectively.

DISCUSSION

A previous study of the multiphase chemistry of pyruvic acid observed products such as zymonic acid not previously seen in PA photochemistry and proposed that the surface of aqueous droplets plays a key role in their production,[17] while a different study noted that PA at the interface is more likely to photochemically form higher-molecular-weight compounds than PA in the bulk.[37] Chemistry leading to oligomerization is especially important for atmospheric chemistry and abiotic synthesis in both contemporary and prebiotic contexts.[11,27,112,113,117−120] Here we used a combination of Langmuir−Blodgett trough experiments and simulation chamber studies to investigate the photochemical and dark chemistry of pyruvic acid that may occur at the surface of water, leading to products not found in the bulk aqueous phase. Additionally, chemistry in bulk water can lead to products that partition to the surface and are collected and analyzed in this work. Both outcomes lead to a modified chemical environment at the air−water interface.

Although pyruvic acid is a relatively soluble organic molecule, it has a higher-than-expected surface activity given its solubility of 10^6 mg/L or 11.4 M.[45] Gordon et al.[45] showed through computational studies that pyruvic acid and also parapyruvic acid and zymonic acid dimers have a positive surface excess, indicating that all three forms partition to the surface to some extent. These computational results are confirmed by vibrational sum frequency generation data also found in Gordon et al.[45] and by the MS data we present here.

A comparison between surface products obtained in the Langmuir−Blodgett trough and those acquired from droplet experiments in the CESAM atmospheric chamber can help illuminate the role of the air−water interface in microdroplet chemistry. Microdroplets produced in the simulation chamber had a number density of 10^5 cm^{-3} with an average diameter of 60 nm, presenting a collective surface area in the simulation chamber of 4.8 × 10^{-3} m^2. The ratio of surface area to bulk volume increases by more than a factor of 1 million in going from the trough to a droplet, providing a unique ability to differentiate surface and bulk chemistry. We expect both experiments to provide enough surface area to reliably observe any product discrepancies between surface and bulk experiments and attribute those differences to the air−water interface.

Information on the surface composition and reactivity of PA is obtained in this study with surface-sensitive methods. Specifically, we utilized a Langmuir trough equipped with a Blodgett dipper to sample species directly from solution surfaces and separately sampled the bulk of the solution, allowing for an internal comparison between the two environments. LEDs were fitted to the trough to study the photochemistry of PA at the air−water interface. This guaranteed that the entire surface area was illuminated, ensuring that efficient and uniform photolysis of the solution was achieved.

Although we studied the interfacial chemistry of PA on flat Langmuir troughs, many of the systems to which we would like to compare and apply our insight into interfacial chemistry are microdroplets or atmospheric aerosols. In view of the size of those systems (diameter ≈ 1 μm) and the molecular lengths of most organic molecules (a few angstroms), the surface area of a droplet is large compared with the area occupied by a molecule (~10^7 times larger). Consequently, the surface is effectively flat, and any effects caused by the curvature of the interface on the reaction mechanism can be neglected.

Indeed, nebulized aqueous PA solution in the simulation chamber CESAM, sampled in real time by PTR-ToF-MS and off-line by ESI-MS of filter samples, largely exhibited the same composition as that observed on the flat trough surface, supporting our assertion that the Langmuir trough can adequately model environmental interfaces. Specifically, lactic acid/lactate and zymonic acid were detected both in CESAM aerosol experiments and in our surface trough experiments in the absence of irradiation. We also saw substantial formation of other oligomers at the surface of the trough experiments, ostensibly from a combination of lactic and pyruvic acid monomers. The most prominent of these oligomers are found at m/z = 161 and 159, possibly corresponding to LA + LA − H_2O and PA + LA − H_2O, respectively, but a series of these oligomers comprising several PA or LA monomers are

https://dx.doi.org/10.1021/acs.jpca.0c09096
J. Phys. Chem. A 2021, 125, 1036−1049

observed. Fu et al.[37] also observed m/z = 159 in their photochemical PA experiments and suggested that it was formed via intramolecular esterification induced by the drying of their bulk liquid sample. They did not detect m/z = 161 or lactic acid.

We propose that the m/z = 159 peak is a PA + LA − H_2O dimer that may be formed by a similar mechanism as zymonic acid, as shown in Scheme 1. It has been proposed elsewhere that after irradiation, the excited pyruvic acid molecule may abstract hydrogen from the methyl group on another PA molecule, forming two radicals that combine to form parapyruvic acid (m/z = 175).[99,102] Parapyruvic acid may then dehydrate to form another detected product (m/z = 157). We propose that the PA + LA − H_2O dimer may form when the excited PA molecule abstracts hydrogen from a LA molecule, forming radicals such as $HA^{\bullet}$ and $LA^{\bullet}$ that then combine and dehydrate to form the dimer product (m/z = 159). Likely structures for both the PA + PA − H_2O and PA + LA − H_2O dimers are shown in Scheme 1. Additional possible structures are shown in Figure S4. Regardless of the exact mechanism of formation, neither lactic acid nor the resulting oligomers are observed in the bulk of the trough solution, suggesting that this phenomenon may be surface-specific. In contrast, the hydrated diol form of pyruvic acid is found only in the bulk.

Zymonic acid has previously been observed as a product of PA photolysis.[17,37] ZA is formed by the combination of two pyruvic acid molecules with the elimination of water, as shown in Scheme 1, pathway A. Since molecules at the air−water interface are partially solvated, they experience a water-restricted environment, so dehydration and therefore dimer formation are likely enhanced at the surface compared with the bulk. Indeed, Reed Harris et al.[17] observed its formation in aqueous PA droplets and suggested that it might be a surface process since ZA had not been detected in bulk PA photolysis, which we corroborate. Fu et al.[37] also observed photochemical production of ZA in both their interfacial and bulk experiments but suggested its presence in their bulk-liquid-phase samples to result from drying of the sample prior to analysis. Zymonic acid has also been previously observed to form from aqueous PA in the dark,[105] but here we present for the first time data showing its presence on the surface of an uncontaminated aqueous PA solution and not in the bulk.

Sui et al. used in situ liquid ToF-SIMS to study glyoxal oxidation at the surface of water with hydrogen peroxide.[55,121] When they compared their liquid ToF-SIMS spectrum to a ToF-SIMS spectrum of a dried glyoxal/peroxide solution, they found several differences, namely, the dried sample exhibited more dehydrated oligomers, while the oligomers observed on the liquid surface tended to be hydrated. We acknowledge that our dipper experiments could be susceptible to an analogous drying effect on the glass slide that enhances the formation of the condensation products (e.g., zymonic acid) that we present here. However, having taken steps to mitigate drying on the slide, having presented an aging experiment in the Langmuir trough (where drying is negligible) in which the condensation products appear to grow in over time, and having observed zymonic acid in an in situ droplet experiment, we believe that it is likely that at least some of the observed oligomers were formed at the water interface prior to our disruption of the system. Regardless, drying may be important to atmospheric aerosol chemistry, as aerosols experience a wide range of humidity and temperature over the course of their life cycle.

Lactic acid is a known product of pyruvic acid photolysis, as shown in Scheme 2.[63,92,99] Here, however, we also observe its

Scheme 2. Photochemical Pathway for Lactic Acid Production from Aqueous Pyruvic Acid[63,a]

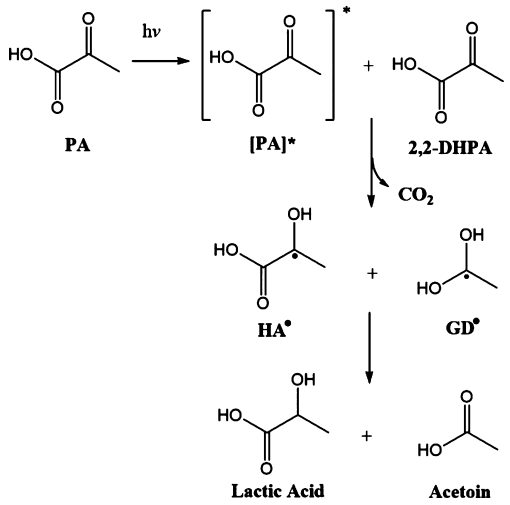

[a]In this case it has been proposed that the excited PA molecule abstracts hydrogen from the acid group of the diol form of PA, 2,2-DHPA, which subsequently loses the CO_2 group to form the $HA^{\bullet}$ and $GD^{\bullet}$ radicals. These radicals then form acetic and lactic acids.

formation in the absence of irradiation. In order to rule out lactic acid as a mere contaminant, we examined NMR data for our purified PA (Figure S1) and did not detect any signal where known chemical shifts of lactic acid would be present. The reduction of pyruvate to lactate in microdroplets was reported by Lee et al.[14] That work implicated the role of the droplet surface, although the solutions used by Lee et al.[14] were more dilute than those used in the present study. The presence of LA or lactate at the surface but not in the bulk in our experiments can be examined in light of the reduction potentials for pyruvate. The bulk aqueous potentials for the reduction of pyruvate to lactate and oxidation of OH^- ions to release electrons are −0.185 V[122] and 2.72 V,[123] respectively. We note that these potentials are bulk values and may change at the air−water interface, where water is much more likely to autoionize.[124−126] However, these values are well within estimates for the surface potential of water. On the basis of previous studies, it has been estimated that a 5 Å air−water interface may create a potential of approximately 3 V, which exceeds the potential necessary to reduce pyruvate.[127,128] Other work from Chamberlayne and Zare[20] and Xiong et al.[21] has shown that the electric double layer of charge in water microdroplets produces an electric field at the surface on the order of 10^7 V/cm, corresponding to a surface potential of 3.63 V. Although this work utilizes flat surfaces in addition to droplets, the electric double layer will also exist on a flat surface, and it is therefore reasonable to expect similar electric fields. Xiong et al.[21] posited that strong fields, like the one they observed, may support spontaneous reduction at the air−water interface.

When we photolyzed aqueous PA solutions, we detected in the bulk the major species predicted by known solution-phase PA photolysis mechanisms, including acetolactic acid, DMTA, and DMOHA.[92,99] These species were also present at the surface but were overshadowed by lactic acid and the

https://dx.doi.org/10.1021/acs.jpca.0c09096
J. Phys. Chem. A 2021, 125, 1036−1049

abundance of LA and PA oligomers. Given that LA and other oligomers were observed in the dark and are also known to form photochemically, it is difficult to quantitatively assess the contributions for each process. Ultimately, however, it is clear that the air−water interface allows for efficient concentration of surface-active oligomers relative to the bulk aqueous solution in both dark and photochemical settings. This generalization is supported by surface area−pressure isotherms measured here and shown in the Figure S2, where the surface activity is clearly enhanced following photolysis. Additionally, nebulized aqueous PA droplets have been shown to become more viscous and grow in size upon photolysis, indicating that similar polymerization reactions occurred.[17]

CONCLUSIONS

The results on the chemistry of PA presented above demonstrate that chemistry at the air−water interface can be very different than that in bulk water, with a strong propensity for oligomer formation at the surface of water. In this study, we used a soluble surfactant, pyruvic acid, which has been well-studied previously in both the gas phase and bulk aqueous solutions with and without exposure to irradiation. Here we investigated its chemistry at the air−water interface using both flat surfaces (Langmuir−Blodgett troughs) and nebulized microdroplets in an atmospheric simulation chamber (CESAM). A comparison of products found at the surface of water and in bulk aqueous solution clearly shows a difference in surface-enhanced products formed under dark and light conditions. Results from dark experiments show that lactic acid/lactate and zymonic acid, a pyruvic acid dimer, are both observed preferentially at the air−water interface. Additionally, we detected a series of higher-molecular-weight oligomers consisting of mixed monomer units of pyruvic and lactic acids, further indicating the tendency of oligomers to reside at the surface of water. When photochemistry is performed, we find that DMTA and DMOHA are more prevalent relative to PA in the bulk than on the surface, while other products, including LA, LA oligomers, and ZA, are observed at the surface.

Because of the prevalence of pyruvic acid in a variety of environments, including the modern atmosphere, prebiotic Earth, and cellular systems, the differences in its chemistry and photochemistry at the air−water interface compared with bulk solution may be important. A previous study showed the impact that mechanistic studies of condensed-phase aqueous pyruvic acid could have on atmospheric modeling:[63] not only did aqueous photolysis rates scale differently than gas-phase rates, a fact not previously taken into account in atmospheric models, but the types of products produced in the aqueous phase led to secondary organic aerosols (SOAs). Another study showed that PA at the interface is susceptible to drying-induced chemistry that differs from bulk photochemistry and produces compounds capable of contributing to aqueous SOA formation.[37] It is likely that the added detail of pyruvic acid chemistry, specifically at the air−water interface, will impact modeling with regard to both the pyruvic acid depletion rates and the formation of SOAs. Furthermore, the production of lactic acid from pyruvic acid is strikingly similar to the role of pyruvic acid in the metabolic cycle. Today, this reduction occurs with enzyme catalysis. However, this work may support the postulate of Lee et al.[14] that this could be a route for prebiotic metabolism. Finally, as Lee et al.[14] also mentioned, the fact that most pyruvic acid chemistry occurs in cells where interfaces are ubiquitous indicates that these studies could have significant implications for cellular chemistry. Regardless, in both modern and prebiotic contexts the surface of water may be an important catalyst for generating chemically complex systems in the natural environment.

ASSOCIATED CONTENT

Supporting Information

The Supporting Information is available free of charge at https://pubs.acs.org/doi/10.1021/acs.jpca.0c09096.

Analytical techniques and instrument parameters: NMR analysis and mass spectrometry; representative ^{1}H NMR spectrum (400 MHz) of purified pyruvic acid in DMSO-d_6; surface pressure−area isotherms of an aqueous solution of 100 mM PA before and after UV irradiation; negative-mode ESI-MS of a zymonic acid standard; negative-mode ESI-MS ion peaks for Langmuir−Blodgett trough control experiments; negative-mode ESI-MS ion peaks of 100 mM aqueous PA before and after photolysis, sampled in the bulk and on the solution surface of a Langmuir−Blodgett trough; ESI-MS comparison of prephotolysis aqueous bulk PA solution and PA droplets; potential structures for the dimers (A) PA + PA − H_2O (m/z = 157) and (B) PA + LA − H_2O (m/z = 159) (PDF)

AUTHOR INFORMATION

Corresponding Author

Veronica Vaida − *Department of Chemistry and Cooperative Institute for Research in Environmental Sciences, University of Colorado Boulder, Boulder, Colorado 80309, United States;* orcid.org/0000-0001-5863-8056; Email: vaida@colorado.edu

Authors

Keaten J. Kappes − *Department of Chemistry and Cooperative Institute for Research in Environmental Sciences, University of Colorado Boulder, Boulder, Colorado 80309, United States;* orcid.org/0000-0001-9951-5407

Alexandra M. Deal − *Department of Chemistry and Cooperative Institute for Research in Environmental Sciences, University of Colorado Boulder, Boulder, Colorado 80309, United States;* orcid.org/0000-0002-1540-9277

Malte F. Jespersen − *Department of Chemistry, University of Copenhagen, DK-2100 Copenhagen, Denmark*

Sandra L. Blair − *Department of Chemistry and Cooperative Institute for Research in Environmental Sciences, University of Colorado Boulder, Boulder, Colorado 80309, United States;* orcid.org/0000-0003-4130-2403

Jean-Francois Doussin − *Laboratoire Interuniversitaire des Systèmes Atmosphériques (LISA), UMR CNRS 7583, Institut Pierre Simon Laplace (IPSL), Université Paris-Est Créteil (UPEC) et Université de Paris (UP), 94010 Creteil, France;* orcid.org/0000-0002-8042-7228

Mathieu Cazaunau − *Laboratoire Interuniversitaire des Systèmes Atmosphériques (LISA), UMR CNRS 7583, Institut Pierre Simon Laplace (IPSL), Université Paris-Est Créteil (UPEC) et Université de Paris (UP), 94010 Creteil, France*

Edouard Pangui − *Laboratoire Interuniversitaire des Systèmes Atmosphériques (LISA), UMR CNRS 7583, Institut Pierre Simon Laplace (IPSL), Université Paris-Est Créteil (UPEC) et Université de Paris (UP), 94010 Creteil, France*

https://dx.doi.org/10.1021/acs.jpca.0c09096
J. Phys. Chem. A 2021, 125, 1036−1049

Brianna N. Hopper − *Department of Chemistry and Cooperative Institute for Research in Environmental Sciences, University of Colorado Boulder, Boulder, Colorado 80309, United States*

Matthew S. Johnson − *Department of Chemistry, University of Copenhagen, DK-2100 Copenhagen, Denmark;* orcid.org/0000-0002-3645-3955

Complete contact information is available at: https://pubs.acs.org/10.1021/acs.jpca.0c09096

Notes

The authors declare no competing financial interest.

■ ACKNOWLEDGMENTS

This work was funded by the U.S. Army Research Office (Grant ARO W911NF1710115) and the National Science Foundation (Grant CHE 1611107). A.M.D. also acknowledges funding from the National Science Foundation Graduate Research Fellowship (Grant DGE 1650115). We also thank the University of Colorado at Boulder Central Analytical Laboratory Mass Spectrometry Core Facility for use of their instruments. The authors gratefully acknowledge CNRS-INSU for supporting CESAM as a national facility and AERIS data center (https://www.aeris-data.fr/) for hosting simulation chamber data.

■ REFERENCES

(1) Carslaw, K. S.; Lee, L. A.; Reddington, C. L.; Pringle, K. J.; Rap, A.; Forster, P. M.; Mann, G. W.; Spracklen, D. V.; Woodhouse, M. T.; Regayre, L. A.; et al. Large contribution of natural aerosols to uncertainty in indirect forcing. *Nature* **2013**, *503* (7474), 67−71.

(2) Donaldson, D. J.; Vaida, V. The influence of organic films at the air-aqueous boundary on atmospheric processes. *Chem. Rev.* **2006**, *106* (4), 1445−61.

(3) Ellison, G. B.; Tuck, A. F.; Vaida, V. Atmospheric processing of organic aerosols. *J. Geophys. Res.: Atmos.* **1999**, *104* (D9), 11633−11641.

(4) Ervens, B.; Carlton, A. G.; Turpin, B. J.; Altieri, K. E.; Kreidenweis, S. M.; Feingold, G. Secondary organic aerosol yields from cloud-processing of isoprene oxidation products. *Geophys. Res. Lett.* **2008**, *35* (2), L02816.

(5) Ruiz-Lopez, M. F.; Francisco, J. S.; Martins-Costa, M. T. C.; Anglada, J. M. Molecular reactions at aqueous interfaces. *Nat. Rev. Chem.* **2020**, *4*, 459−475.

(6) Stevens, B.; Feingold, G. Untangling aerosol effects on clouds and precipitation in a buffered system. *Nature* **2009**, *461* (7264), 607−13.

(7) Tang, M.; Cziczo, D. J.; Grassian, V. H. Interactions of water with mineral dust aerosol: Water adsorption, hygroscopicity, cloud condensation, and ice nucleation. *Chem. Rev.* **2016**, *116* (7), 4205−59.

(8) Zhong, J.; Kumar, M.; Anglada, J. M.; Martins-Costa, M. T. C.; Ruiz-Lopez, M. F.; Zeng, X. C.; Francisco, J. S. Atmospheric spectroscopy and photochemistry at environmental water interfaces. *Annu. Rev. Phys. Chem.* **2019**, *70*, 45−69.

(9) George, C.; Ammann, M.; D'Anna, B.; Donaldson, D. J.; Nizkorodov, S. A. Heterogeneous photochemistry in the atmosphere. *Chem. Rev.* **2015**, *115* (10), 4218−4258.

(10) Banerjee, S.; Gnanamani, E.; Yan, X.; Zare, R. N. Can all bulk-phase reactions be accelerated in microdroplets? *Analyst* **2017**, *142* (9), 1399−1402.

(11) Dobson, C. M.; Ellison, G. B.; Tuck, A. F.; Vaida, V. Atmospheric aerosols as prebiotic chemical reactors. *Proc. Natl. Acad. Sci. U. S. A.* **2000**, *97* (22), 11864−8.

(12) Griffith, E. C.; Vaida, V. In situ observation of peptide bond formation at the water-air interface. *Proc. Natl. Acad. Sci. U. S. A.* **2012**, *109* (39), 15697−701.

(13) Lee, J. K.; Banerjee, S.; Nam, H. G.; Zare, R. N. Acceleration of reaction in charged microdroplets. *Q. Rev. Biophys.* **2015**, *48* (4), 437−44.

(14) Lee, J. K.; Samanta, D.; Nam, H. G.; Zare, R. N. Micrometer-sized water droplets induce spontaneous reduction. *J. Am. Chem. Soc.* **2019**, *141* (27), 10585−10589.

(15) Marsh, B. M.; Iyer, K.; Cooks, R. G. Reaction acceleration in electrospray droplets: Size, distance, and surfactant effects. *J. Am. Soc. Mass Spectrom.* **2019**, *30* (10), 2022−2030.

(16) Nam, I.; Lee, J. K.; Nam, H. G.; Zare, R. N. Abiotic production of sugar phosphates and uridine ribonucleoside in aqueous microdroplets. *Proc. Natl. Acad. Sci. U. S. A.* **2017**, *114* (47), 12396−12400.

(17) Reed Harris, A. E.; Pajunoja, A.; Cazaunau, M.; Gratien, A.; Pangui, E.; Monod, A.; Griffith, E. C.; Virtanen, A.; Doussin, J. F.; Vaida, V. Multiphase photochemistry of pyruvic acid under atmospheric conditions. *J. Phys. Chem. A* **2017**, *121* (18), 3327−3339.

(18) Rossignol, S.; Tinel, L.; Bianco, A.; Passananti, M.; Brigante, M.; Donaldson, D. J.; George, C. Atmospheric photochemistry at a fatty acid-coated air-water interface. *Science* **2016**, *353* (6300), 699−702.

(19) Griffith, E. C.; Vaida, V. Ionization state of L-phenylalanine at the air-water interface. *J. Am. Chem. Soc.* **2013**, *135* (2), 710−716.

(20) Chamberlayne, C. F.; Zare, R. N. Simple model for the electric field and spatial distribution of ions in a microdroplet. *J. Chem. Phys.* **2020**, *152* (18), 184702.

(21) Xiong, H.; Lee, J. K.; Zare, R. N.; Min, W. Strong electric field observed at the interface of aqueous microdroplets. *J. Phys. Chem. Lett.* **2020**, *11* (17), 7423−7428.

(22) Seinfeld, J. H.; Pandis, S. N. *Atmospheric Chemistry and Physics: From Air Pollution to Climate Change*; John Wiley & Sons, 2016.

(23) Finlayson-Pitts, B. J.; Pitts, J. N., Jr. *Chemistry of the Upper and Lower Atmosphere: Theory, Experiments, and Applications*; Elsevier, 1999.

(24) Donaldson, D.; Valsaraj, K. T. Adsorption and reaction of trace gas-phase organic compounds on atmospheric water film surfaces: A critical review. *Environ. Sci. Technol.* **2010**, *44* (3), 865−873.

(25) Ervens, B.; Turpin, B. J.; Weber, R. J. Secondary organic aerosol formation in cloud droplets and aqueous particles (aqSOA): A review of laboratory, field and model studies. *Atmos. Chem. Phys.* **2011**, *11* (21), 11069−11102.

(26) Pezzotti, S.; Galimberti, D. R.; Gaigeot, M.-P. 2D H-bond network as the topmost skin to the air−water interface. *J. Phys. Chem. Lett.* **2017**, *8* (13), 3133−3141.

(27) Griffith, E. C.; Tuck, A. F.; Vaida, V. Ocean-atmosphere interactions in the emergence of complexity in simple chemical systems. *Acc. Chem. Res.* **2012**, *45* (12), 2106−2113.

(28) Mompeán, C.; Marín-Yaseli, M. R.; Espigares, P.; González-Toril, E.; Zorzano, M. P.; Ruiz-Bermejo, M. Prebiotic chemistry in neutral/reduced-alkaline gas-liquid interfaces. *Sci. Rep.* **2019**, *9*, 1916.

(29) Powner, M. W.; Gerland, B.; Sutherland, J. D. Synthesis of activated pyrimidine ribonucleotides in prebiotically plausible conditions. *Nature* **2009**, *459* (7244), 239−42.

(30) Tuck, A. The role of atmospheric aerosols in the origin of life. *Surv. Geophy.* **2002**, *23* (5), 379−409.

(31) Tuck, A. F. Proposed empirical entropy and gibbs energy based on observations of scale invariance in open nonequilibrium systems. *J. Phys. Chem. A* **2017**, *121* (35), 6620−6629.

(32) Mason, B. Bursting of air bubbles at the surface of sea water. *Nature* **1954**, *174* (4427), 470−471.

(33) Tuck, A. F. Gibbs free energy and reaction rate acceleration in and on microdroplets. *Entropy* **2019**, *21* (11), 1044.

(34) Alpert, P. A.; Ciuraru, R.; Rossignol, S.; Passananti, M.; Tinel, L.; Perrier, S.; Dupart, Y.; Steimer, S. S.; Ammann, M.; Donaldson, D. J.; George, C. Fatty acid surfactant photochemistry results in new particle formation. *Sci. Rep.* **2017**, *7* (1), 12693.

(35) Altieri, K. E.; Carlton, A. G.; Lim, H. J.; Turpin, B. J.; Seitzinger, S. P. Evidence for oligomer formation in clouds: Reactions of isoprene oxidation products. *Environ. Sci. Technol.* **2006**, *40* (16), 4956−4960.
(36) Fang, Y.; Riahi, S.; McDonald, A. T.; Shrestha, M.; Tobias, D. J.; Grassian, V. H. What is the driving force behind the adsorption of hydrophobic molecules on hydrophilic surfaces? *J. Phys. Chem. Lett.* **2019**, *10* (3), 468−473.
(37) Fu, Y.; Zhang, Y.; Zhang, F.; Chen, J.; Zhu, Z.; Yu, X.-Y. Does interfacial photochemistry play a role in the photolysis of pyruvic acid in water? *Atmos. Environ.* **2018**, *191*, 36−45.
(38) Gao, S.; Ng, N. L.; Keywood, M.; Varutbangkul, V.; Bahreini, R.; Nenes, A.; He, J.; Yoo, K. Y.; Beauchamp, J.; Hodyss, R. P.; et al. Particle phase acidity and oligomer formation in secondary organic aerosol. *Environ. Sci. Technol.* **2004**, *38* (24), 6582−6589.
(39) Kalberer, M.; Paulsen, D.; Sax, M.; Steinbacher, M.; Dommen, J.; Prévôt, A. S.; Fisseha, R.; Weingartner, E.; Frankevich, V.; Zenobi, R. Identification of polymers as major components of atmospheric organic aerosols. *Science* **2004**, *303* (5664), 1659−1662.
(40) Reddy, S. K.; Thiraux, R.; Wellen Rudd, B. A.; Lin, L.; Adel, T.; Joutsuka, T.; Geiger, F. M.; Allen, H. C.; Morita, A.; Paesani, F. Bulk contributions modulate the sum-frequency generation spectra of water on model sea-spray aerosols. *Chem.* **2018**, *4* (7), 1629−1644.
(41) Tolocka, M. P.; Jang, M.; Ginter, J. M.; Cox, F. J.; Kamens, R. M.; Johnston, M. V. Formation of oligomers in secondary organic aerosol. *Environ. Sci. Technol.* **2004**, *38* (5), 1428−1434.
(42) Trueblood, J. V.; Alves, M. R.; Power, D.; Santander, M. V.; Cochran, R. E.; Prather, K. A.; Grassian, V. H. Shedding light on photosensitized reactions within marine-relevant organic thin films. *ACS Earth Space Chem.* **2019**, *3* (8), 1614−1623.
(43) Eisenthal, K. Liquid interfaces probed by second-harmonic and sum-frequency spectroscopy. *Chem. Rev.* **1996**, *96* (4), 1343−1360.
(44) Geissler, P. L. Water interfaces, solvation, and spectroscopy. *Annu. Rev. Phys. Chem.* **2013**, *64*, 317−37.
(45) Gordon, B. P.; Moore, F. G.; Scatena, L. F.; Richmond, G. L. On the rise: Experimental and computational vibrational sum frequency spectroscopy studies of pyruvic acid and its surface active oligomer species at the air-water interface. *J. Phys. Chem. A* **2019**, *123* (49), 10609−10619.
(46) Jungwirth, P.; Tobias, D. J. Ions at the air/water interface. *J. Phys. Chem. B* **2002**, *106* (25), 6361−6373.
(47) Medders, G. R.; Paesani, F. Dissecting the molecular structure of the air/water interface from quantum simulations of the sum-frequency generation spectrum. *J. Am. Chem. Soc.* **2016**, *138* (11), 3912−9.
(48) Morita, A.; Hynes, J. T. A theoretical analysis of the sum frequency generation spectrum of the water surface. *Chem. Phys.* **2000**, *258* (2−3), 371−390.
(49) Mucha, M.; Frigato, T.; Levering, L. M.; Allen, H. C.; Tobias, D. J.; Dang, L. X.; Jungwirth, P. Unified molecular picture of the surfaces of aqueous acid, base, and salt solutions. *J. Phys. Chem. B* **2005**, *109* (16), 7617−23.
(50) Qian, Y.; Deng, G.-h.; Rao, Y. In situ spectroscopic probing of polarity and molecular configuration at aerosol particle surfaces. *J. Phys. Chem. Lett.* **2020**, *11* (16), 6763−6771.
(51) Richmond, G. Molecular bonding and interactions at aqueous surfaces as probed by vibrational sum frequency spectroscopy. *Chem. Rev.* **2002**, *102* (8), 2693−2724.
(52) Scatena, L.; Brown, M.; Richmond, G. Water at hydrophobic surfaces: Weak hydrogen bonding and strong orientation effects. *Science* **2001**, *292* (5518), 908−912.
(53) Shen, Y. R.; Ostroverkhov, V. Sum-frequency vibrational spectroscopy on water interfaces: Polar orientation of water molecules at interfaces. *Chem. Rev.* **2006**, *106* (4), 1140−1154.
(54) Verreault, D.; Hua, W.; Allen, H. C. From conventional to phase-sensitive vibrational sum frequency generation spectroscopy: Probing water organization at aqueous interfaces. *J. Phys. Chem. Lett.* **2012**, *3* (20), 3012−3028.
(55) Sui, X.; Zhou, Y.; Zhang, F.; Chen, J.; Zhu, Z.; Yu, X.-Y. Deciphering the aqueous chemistry of glyoxal oxidation with hydrogen peroxide using molecular imaging. *Phys. Chem. Chem. Phys.* **2017**, *19* (31), 20357−20366.
(56) Zhang, F.; Yu, X.; Chen, J.; Zhu, Z.; Yu, X.-Y. Dark air−liquid interfacial chemistry of glyoxal and hydrogen peroxide. *npj Clim. Atmos. Sci.* **2019**, *2* (1), 28.
(57) Zhang, F.; Yu, X.; Sui, X.; Chen, J.; Zhu, Z.; Yu, X.-Y. Evolution of aqsoa from the air−liquid interfacial photochemistry of glyoxal and hydroxyl radicals. *Environ. Sci. Technol.* **2019**, *53* (17), 10236−10245.
(58) Tervahattu, H.; Juhanoja, J.; Kupiainen, K. Identification of an organic coating on marine aerosol particles by TOF-SIMS. *J. Geophys. Res.* **2002**, *107* (D16), ACH 18-1−ACH 18-7.
(59) Tervahattu, H.; Juhanoja, J.; Vaida, V.; Tuck, A. F.; Niemi, J. V.; Kupiainen, K.; Kulmala, M.; Vehkamäki, H. Fatty acids on continental sulfate aerosol particles. *J. Geophys. Res.: Atmos.* **2005**, *110* (D6), D06207.
(60) Kumar, J. K.; Oliver, J. S. Proximity effects in monolayer films: Kinetic analysis of amide bond formation at the air− water interface using ^{1}H NMR spectroscopy. *J. Am. Chem. Soc.* **2002**, *124* (38), 11307−11314.
(61) Ciuraru, R.; Fine, L.; Van Pinxteren, M.; D'Anna, B.; Herrmann, H.; George, C. Photosensitized production of functionalized and unsaturated organic compounds at the air-sea interface. *Sci. Rep.* **2015**, *5*, 12741.
(62) Fu, H.; Ciuraru, R.; Dupart, Y.; Passananti, M.; Tinel, L.; Rossignol, S. p.; Perrier, S.; Donaldson, D. J.; Chen, J.; George, C. Photosensitized production of atmospherically reactive organic compounds at the air/aqueous interface. *J. Am. Chem. Soc.* **2015**, *137* (26), 8348−8351.
(63) Reed Harris, A. E.; Ervens, B.; Shoemaker, R. K.; Kroll, J. A.; Rapf, R. J.; Griffith, E. C.; Monod, A.; Vaida, V. Photochemical kinetics of pyruvic acid in aqueous solution. *J. Phys. Chem. A* **2014**, *118* (37), 8505−8516.
(64) Renard, P.; Reed Harris, A. E.; Rapf, R. J.; Ravier, S.; Demelas, C.; Coulomb, B.; Quivet, E.; Vaida, V.; Monod, A. Aqueous phase oligomerization of methyl vinyl ketone by atmospheric radical reactions. *J. Phys. Chem. C* **2014**, *118* (50), 29421−29430.
(65) Shrestha, M.; Luo, M.; Li, Y.; Xiang, B.; Xiong, W.; Grassian, V. H. Let there be light: Stability of palmitic acid monolayers at the air/salt water interface in the presence and absence of simulated solar light and a photosensitizer. *Chem. Sci.* **2018**, *9* (26), 5716−5723.
(66) Vaida, V. Atmospheric radical chemistry revisited. *Science* **2016**, *353* (6300), 650−650.
(67) Andreae, M. O.; Talbot, R. W.; Li, S. M. Atmospheric measurements of pyruvic and formic-acid. *J. Geophys. Res.* **1987**, *92* (D6), 6635−6641.
(68) Eger, P. G.; Schuladen, J.; Sobanski, N.; Fischer, H.; Karu, E.; Williams, J.; Riva, M.; Zha, Q.; Ehn, M.; Quéléver, L. L.; et al. Pyruvic acid in the boreal forest: Gas-phase mixing ratios and impact on radical chemistry. *Atmos. Chem. Phys.* **2020**, *20* (6), 3697−3711.
(69) Guzmán, M.; Hoffmann, M.; Colussi, A. Photolysis of pyruvic acid in ice: Possible relevance to co and co2 ice core record anomalies. *J. Geophys. Res.: Atmos.* **2007**, *112* (D10), D10123.
(70) Shiraiwa, M.; Zuend, A.; Bertram, A. K.; Seinfeld, J. H. Gas−particle partitioning of atmospheric aerosols: Interplay of physical state, non-ideal mixing and morphology. *Phys. Chem. Chem. Phys.* **2013**, *15* (27), 11441−11453.
(71) Cody, G. D.; Boctor, N. Z.; Filley, T. R.; Hazen, R. M.; Scott, J. H.; Sharma, A.; Yoder, H. S. Primordial carbonylated iron-sulfur compounds and the synthesis of pyruvate. *Science* **2000**, *289* (5483), 1337−1340.
(72) Cooper, G.; Reed, C.; Nguyen, D.; Carter, M.; Wang, Y. Detection and formation scenario of citric acid, pyruvic acid, and other possible metabolism precursors in carbonaceous meteorites. *Proc. Natl. Acad. Sci. U. S. A.* **2011**, *108* (34), 14015−14020.
(73) Griffith, E. C.; Shoemaker, R. K.; Vaida, V. Sunlight-initiated chemistry of aqueous pyruvic acid: Building complexity in the origin of life. *Origins Life Evol. Biospheres* **2013**, *43* (4−5), 341−352.

https://dx.doi.org/10.1021/acs.jpca.0c09096
J. Phys. Chem. A 2021, 125, 1036−1049

(74) Guzman, M. I.; Martin, S. T. Prebiotic metabolism: Production by mineral photoelectrochemistry of α-ketocarboxylic acids in the reductive tricarboxylic acid cycle. *Astrobiology* **2009**, *9* (9), 833−842.
(75) Pizzarello, S.; Shock, E. The organic composition of carbonaceous meteorites: The evolutionary story ahead of biochemistry. *Cold Spring Harbor Perspect. Biol.* **2010**, *2* (3), a002105.
(76) Shapiro, R. Small molecule interactions were central to the origin of life. *Q. Rev. Biol.* **2006**, *81* (2), 105−125.
(77) Berges, M. G.; Warneck, P. Product quantum yields for the 350 nm photodecomposition of pyruvic acid in air. *Ber. Bunsen-Ges. Phys. Chem.* **1992**, *96* (3), 413−416.
(78) Grosjean, D. Atmospheric reactions of pyruvic acid. *Atmos. Environ. (1967-1989)* **1983**, *17* (11), 2379−2382.
(79) Reed Harris, A. E.; Cazaunau, M.; Gratien, A.; Pangui, E.; Doussin, J. F.; Vaida, V. Atmospheric simulation chamber studies of the gas-phase photolysis of pyruvic acid. *J. Phys. Chem. A* **2017**, *121* (44), 8348−8358.
(80) Leermakers, P. A.; Vesley, G. F. The photochemistry of α-keto acids and α-keto esters. I. Photolysis of pyruvic acid and benzoylformic acid. *J. Am. Chem. Soc.* **1963**, *85* (23), 3776−3779.
(81) Mellouki, A.; Mu, Y. On the atmospheric degradation of pyruvic acid in the gas phase. *J. Photochem. Photobiol., A* **2003**, *157* (2−3), 295−300.
(82) Reed Harris, A. E.; Doussin, J. F.; Carpenter, B. K.; Vaida, V. Gas-phase photolysis of pyruvic acid: The effect of pressure on reaction rates and products. *J. Phys. Chem. A* **2016**, *120* (51), 10123−10133.
(83) Sutradhar, S.; Samanta, B. R.; Fernando, R.; Reisler, H. Spectroscopy and two-photon dissociation of jet-cooled pyruvic acid. *J. Phys. Chem. A* **2019**, *123* (28), 5906−5917.
(84) Takahashi, K.; Plath, K. L.; Skodje, R. T.; Vaida, V. Dynamics of vibrational overtone excited pyruvic acid in the gas phase: Line broadening through hydrogen-atom chattering. *J. Phys. Chem. A* **2008**, *112* (32), 7321−7331.
(85) Vesley, G. F.; Leermakers, P. A. The photochemistry of α-keto acids and α-keto esters. Iii. Photolysis of pyruvic acid in the vapor phase. *J. Phys. Chem.* **1964**, *68* (8), 2364−2366.
(86) Yamamoto, S.; Back, R. A. The photolysis and thermal-decomposition of pyruvic-acid in the gas-phase. *Can. J. Chem.* **1985**, *63* (2), 549−554.
(87) Church, J. R.; Vaida, V.; Skodje, R. T. Gas-phase reaction kinetics of pyruvic acid with oh radicals: The role of tunneling, complex formation, and conformational structure. *J. Phys. Chem. A* **2020**, *124* (5), 790−800.
(88) Chang, X.-P.; Fang, Q.; Cui, G. Mechanistic photodecarboxylation of pyruvic acid: Excited-state proton transfer and three-state intersection. *J. Chem. Phys.* **2014**, *141* (15), 154311.
(89) da Silva, G. Decomposition of pyruvic acid on the ground-state potential energy surface. *J. Phys. Chem. A* **2016**, *120* (2), 276−283.
(90) Eugene, A. J.; Guzman, M. I. Reactivity of ketyl and acetyl radicals from direct solar actinic photolysis of aqueous pyruvic acid. *J. Phys. Chem. A* **2017**, *121* (15), 2924−2935.
(91) Eugene, A. J.; Guzman, M. I. The effects of reactant concentration and air flow rate in the consumption of dissolved O_2 during the photochemistry of aqueous pyruvic acid. *Molecules* **2019**, *24* (6), 1124.
(92) Griffith, E. C.; Carpenter, B. K.; Shoemaker, R. K.; Vaida, V. Photochemistry of aqueous pyruvic acid. *Proc. Natl. Acad. Sci. U. S. A.* **2013**, *110* (29), 11714−11719.
(93) Griffith, E. C.; Carpenter, B. K.; Shoemaker, R. K.; Vaida, V. Reply to eugene et al.: Photochemistry of aqueous pyruvic acid. *Proc. Natl. Acad. Sci. U. S. A.* **2013**, *110* (46), E4276−E4276.
(94) Griffith, E. C.; Rapf, R. J.; Shoemaker, R. K.; Carpenter, B. K.; Vaida, V. Photoinitiated synthesis of self-assembled vesicles. *J. Am. Chem. Soc.* **2014**, *136* (10), 3784−3787.
(95) Guzman, M. I.; Colussi, A. J.; Hoffmann, M. R. Photoinduced oligomerization of aqueous pyruvic acid. *J. Phys. Chem. A* **2006**, *110* (10), 3619−3626.
(96) Larsen, M. C.; Vaida, V. Near infrared photochemistry of pyruvic acid in aqueous solution. *J. Phys. Chem. A* **2012**, *116* (24), 5840−5846.
(97) Leermakers, P.; Vesley, G. Photolysis of pyruvic acid in solution. *J. Org. Chem.* **1963**, *28* (4), 1160−1161.
(98) Mekic, M.; Brigante, M.; Vione, D.; Gligorovski, S. Exploring the ionic strength effects on the photochemical degradation of pyruvic acid in atmospheric deliquescent aerosol particles. *Atmos. Environ.* **2018**, *185*, 237−242.
(99) Rapf, R. J.; Perkins, R. J.; Carpenter, B. K.; Vaida, V. Mechanistic description of photochemical oligomer formation from aqueous pyruvic acid. *J. Phys. Chem. A* **2017**, *121* (22), 4272−4282.
(100) Davidson, R. S.; Goodwin, D.; De Violet, P. F. The mechanism of the photo-induced decarboxylatton of pyruvic acid in solution. *Chem. Phys. Lett.* **1981**, *78* (3), 471−474.
(101) Guzman, M.; Colussi, A.; Hoffmann, M. Photoinduced oligomerization of aqueous pyruvic acid. *J. Phys. Chem. A* **2006**, *110* (10), 3619−3626.
(102) Rapf, R. J.; Dooley, M. R.; Kappes, K.; Perkins, R. J.; Vaida, V. Ph dependence of the aqueous photochemistry of alpha-keto acids. *J. Phys. Chem. A* **2017**, *121* (44), 8368−8379.
(103) Rincón, A. G.; Guzmán, M. I.; Hoffmann, M. R.; Colussi, A. Optical absorptivity versus molecular composition of model organic aerosol matter. *J. Phys. Chem. A* **2009**, *113* (39), 10512−10520.
(104) Wang, J.; Doussin, J. F.; Perrier, S.; Perraudin, E.; Katrib, Y.; Pangui, E.; Picquet-Varrault, B. Design of a new multi-phase experimental simulation chamber for atmospheric photosmog, aerosol and cloud chemistry research. *Atmos. Meas. Tech.* **2011**, *4* (11), 2465−2494.
(105) Perkins, R. J.; Shoemaker, R. K.; Carpenter, B. K.; Vaida, V. Chemical equilibria and kinetics in aqueous solutions of zymonic acid. *J. Phys. Chem. A* **2016**, *120* (51), 10096−10107.
(106) Eliason, T. L.; Gilman, J. B.; Vaida, V. Oxidation of organic films relevant to atmospheric aerosols. *Atmos. Environ.* **2004**, *38* (9), 1367−1378.
(107) Gilman, J. B.; Eliason, T. L.; Fast, A.; Vaida, V. Selectivity and stability of organic films at the air-aqueous interface. *J. Colloid Interface Sci.* **2004**, *280* (1), 234−243.
(108) Griffith, E. C.; Adams, E. M.; Allen, H. C.; Vaida, V. Hydrophobic collapse of a stearic acid film by adsorbed l-phenylalanine at the air-water interface. *J. Phys. Chem. B* **2012**, *116* (27), 7849−7857.
(109) Griffith, E. C.; Guizado, T. R. C.; Pimentel, A. S.; Tyndall, G. S.; Vaida, V. Oxidized aromatic−aliphatic mixed films at the air−aqueous solution interface. *J. Phys. Chem. C* **2013**, *117* (43), 22341−22350.
(110) Griffith, E. C.; Perkins, R. J.; Telesford, D. M.; Adams, E. M.; Cwiklik, L.; Allen, H. C.; Roeselová, M.; Vaida, V. Interaction of L-phenylalanine with a phospholipid monolayer at the water−air interface. *J. Phys. Chem. B* **2015**, *119* (29), 9038−9048.
(111) Perkins, R. J.; Kukharchuk, A.; Delcroix, P.; Shoemaker, R. K.; Roeselova, M.; Cwiklik, L.; Vaida, V. The partitioning of small aromatic molecules to air-water and phospholipid interfaces mediated by non-hydrophobic interactions. *J. Phys. Chem. B* **2016**, *120* (30), 7408−7422.
(112) Rapf, R.; Griffith, E.; Vaida, V. Sunlight-driven synthesis and self-assembly of a model amphiphile at the air-water interface. *Abstr. Pap. - Am. Chem. Soc.* **2015**, *249*, ENVR 62.
(113) Rapf, R. J.; Perkins, R. J.; Yang, H. S.; Miyake, G.; Carpenter, B. K.; Vaida, V. Photochemical synthesis of oligomeric amphiphiles from alkyl oxoacids in aqueous environments. *J. Am. Chem. Soc.* **2017**, *139* (20), 6946−6959.
(114) Bregonzio-Rozier, L.; Siekmann, F.; Giorio, C.; Pangui, E.; Morales, S. B.; Temime-Roussel, B.; Gratien, A.; Michoud, V.; Ravier, S.; Cazaunau, M.; et al. Gaseous products and secondary organic aerosol formation during long term oxidation of isoprene and methacrolein. *Atmos. Chem. Phys.* **2015**, *15* (6), 2953−2968.
(115) Kramer, Z. C.; Takahashi, K.; Vaida, V.; Skodje, R. T. Will water act as a photocatalyst for cluster phase chemical reactions?

https://dx.doi.org/10.1021/acs.jpca.0c09096
J. Phys. Chem. A 2021, 125, 1036−1049

Vibrational overtone-induced dehydration reaction of methanediol. *J. Chem. Phys.* **2012**, *136* (16), 164302.
(116) Maroń, M. K.; Takahashi, K.; Shoemaker, R. K.; Vaida, V. Hydration of pyruvic acid to its geminal-diol, 2, 2-dihydroxypropanoic acid, in a water-restricted environment. *Chem. Phys. Lett.* **2011**, *513* (4−6), 184−190.
(117) Donaldson, D. J.; Tervahattu, H.; Tuck, A. F.; Vaida, V. Organic aerosols and the origin of life: An hypothesis. *Origins Life Evol. Biospheres* **2004**, *34* (1−2), 57−67.
(118) Donaldson, D. J.; Tuck, A. F.; Vaida, V. The asymmetry of organic aerosol fission and prebiotic chemistry. *Origins Life Evol. Biospheres* **2002**, *32* (3), 237−245.
(119) Vaida, V. Ocean sea spray, clouds, and climate. *ACS Cent. Sci.* **2015**, *1* (3), 112−114.
(120) Vaida, V. Prebiotic phosphorylation enabled by microdroplets. *Proc. Natl. Acad. Sci. U. S. A.* **2017**, *114* (47), 12359−12361.
(121) Sui, X.; Zhou, Y.; Zhang, F.; Zhang, Y.; Chen, J.; Zhu, Z.; Yu, X. Y. Tof-sims characterization of glyoxal surface oxidation products by hydrogen peroxide: A comparison between dry and liquid samples. *Surf. Interface Anal.* **2018**, *50* (10), 927−938.
(122) Karp, G. *Cell and Molecular Biology: Concepts and Experiments*; John Wiley & Sons, 2009.
(123) Schwarz, H. A.; Dodson, R. W. Equilibrium between hydroxyl radicals and thallium(ii) and the oxidation potential of oh(aq). *J. Phys. Chem.* **1984**, *88* (16), 3643−3647.
(124) Agmon, N.; Bakker, H. J.; Campen, R. K.; Henchman, R. H.; Pohl, P.; Roke, S.; Thamer, M.; Hassanali, A. Protons and hydroxide ions in aqueous systems. *Chem. Rev.* **2016**, *116* (13), 7642−72.
(125) Buch, V.; Milet, A.; Vacha, R.; Jungwirth, P.; Devlin, J. P. Water surface is acidic. *Proc. Natl. Acad. Sci. U. S. A.* **2007**, *104* (18), 7342−7347.
(126) Tse, Y. L.; Chen, C.; Lindberg, G. E.; Kumar, R.; Voth, G. A. Propensity of hydrated excess protons and hydroxide anions for the air-water interface. *J. Am. Chem. Soc.* **2015**, *137* (39), 12610−6.
(127) Kathmann, S. M.; Kuo, I. F. W.; Mundy, C. J. Electronic effects on the surface potential at the vapor-liquid interface of water (vol 130, 16556, 2008). *J. Am. Chem. Soc.* **2009**, *131* (47), 17522−17522.
(128) Paluch, M. Surface potential at the water-air interface. *Ann. Univ. Mariae Curie-Sklodowska, Sect. AA: Chem.* **2015**, *70* (2), 1−11.

https://dx.doi.org/10.1021/acs.jpca.0c09096
J. Phys. Chem. A 2021, 125, 1036−1049